The phospho–caveolin-1 scaffolding domain dampens force fluctuations in focal adhesions and promotes cancer cell migration

Fanrui Meng[a], Sandeep Saxena[a], Youtao Liu[a], Bharat Joshi[a], Timothy H. Wong[a], Jay Shankar[a], Leonard J. Foster[b], Pascal Bernatchez[c,d], and Ivan R. Nabi[a,*]

[a]Department of Cellular and Physiological Sciences, Life Sciences Institute, [b]Department of Biochemistry and Molecular Biology and Michael Smith Labs, and [d]Department of Anesthesiology, Pharmacology and Therapeutics, University of British Columbia, Vancouver, BC V6T 1Z3, Canada; [c]James Hogg Research Centre, Institute for Heart + Lung Health, St Paul's Hospital, Vancouver, BC V6Z 1Y6, Canada

ABSTRACT **Caveolin-1 (Cav1), a major Src kinase substrate phosphorylated on tyrosine-14 (Y14), contains the highly conserved membrane-proximal caveolin scaffolding domain (CSD; amino acids 82–101). Here we show, using CSD mutants (F92A/V94A) and membrane-permeable CSD-competing peptides, that Src kinase–dependent pY14Cav1 regulation of focal adhesion protein stabilization, focal adhesion tension, and cancer cell migration is CSD dependent. Quantitative proteomic analysis of Cav1-GST (amino acids 1–101) pull downs showed sixfold-increased binding of vinculin and, to a lesser extent, α-actinin, talin, and filamin, to phosphomimetic Cav1Y14D relative to nonphosphorylatable Cav1Y14F. Consistently, pY14Cav1 enhanced CSD-dependent vinculin tension in focal adhesions, dampening force fluctuation and synchronously stabilizing cellular focal adhesions in a high-tension mode, paralleling effects of actin stabilization. This identifies pY14Cav1 as a molecular regulator of focal adhesion tension and suggests that functional interaction between Cav1 Y14 phosphorylation and the CSD promotes focal adhesion traction and, thereby, cancer cell motility.**

Monitoring Editor
Asma Nusrat
Emory University

Received: May 5, 2017
Accepted: Jun 2, 2017

INTRODUCTION

Focal adhesions are macromolecular complexes in which transmembrane integrins and cytoplasmic proteins, including vinculin, talin, α-actinin, and focal adhesion kinase (FAK), link the extracellular matrix (ECM) to the actin cytoskeleton (Burridge *et al.*, 1988; Gardel *et al.*, 2010; Case and Waterman, 2015). Focal adhesions are key transmitters of the cellular response to mechanical force upon actomyosin contractility and ECM rigidity (Hoffman, 2014; Burridge and Guilluy, 2016). Vinculin, a cytoplasmic component of focal adhesions, interacts with both the talin–integrin complex and the actin cytoskeleton and is closely involved in focal adhesion tension-induced signaling (Cohen *et al.*, 2006; Ziegler *et al.*, 2006; del Rio *et al.*, 2009; Kanchanawong *et al.*, 2010; Carisey *et al.*, 2013). On activation at sites of cell adhesion, vinculin switches from a closed, globular conformation to an extended conformation allowing binding of specific partners to the head (Vh) and tail (Vt) domains (Bakolitsa *et al.*, 2004; Cohen *et al.*, 2006; Ziegler *et al.*, 2006). Active extended vinculin stabilizes various focal adhesion proteins, including FAK, within focal adhesions and activates integrins in an actin- and talin-dependent manner (Carisey *et al.*, 2013). A fluorescence resonance energy transfer (FRET)–based vinculin tension sensor (VinTS) construct showed that force transmission across vinculin is selectively enhanced in leading-edge focal adhesions and determines focal adhesion size and turnover (Grashoff *et al.*, 2010; Hernandez-Varas *et al.*, 2015).

Src kinase is a key regulator of focal adhesion signaling, phosphorylating multiple focal adhesion proteins, including FAK and vinculin, and also tumor cell migration. Integrin-dependent autophosphorylation of FAK tyrosine 397 (Y397) creates a high-affinity

This article was published online ahead of print in MBoC in Press (http://www.molbiolcell.org/cgi/doi/10.1091/mbc.E17-05-0278) on June 7, 2017.

*Address correspondence to: Ivan R. Nabi (irnabi@mail.ubc.ca).

Abbreviations used: AP, antennapedia; AP-Cav, AP fused to the CSD sequence; Cav1, caveolin-1; CSD, caveolin scaffolding domain; ECM, extracellular matrix; EGFP, enhanced green fluorescent protein; eNOS, endothelial nitric oxide synthase; FA, focal adhesion; FAK, focal adhesion kinase; FN, fibronectin; FRAP, fluorescence recovery after photobleaching; FRET, fluorescence resonance energy transfer; FRET SE, sensitized emission FRET; GST, glutathione-*S*-transferase; mRFP, monomeric red fluorescent protein; PBS/CM, PBS plus 0.1 mM Ca^{2+} and 1 mM Mg^{2+}; pY14Cav1, Y14 phosphorylated Cav1; SH2, Src homology 2; Vh, vinculin head domain; VinTS, vinculin tension sensor; Vt, vinculin tail domain.

binding site for Src homology 2 (SH2)–containing proteins, including Src kinase (Mitra and Schlaepfer, 2006). FAK-Src signaling is a key regulator of the dynamic recruitment of focal adhesion components and leading-edge activity (Webb *et al.*, 2004). Src phosphorylation of tyrosine 1065 (Y1065) of vinculin induces its conformation-based activation and tension (Zhang *et al.*, 2004; Huang *et al.*, 2014). Curiously, the major Src tyrosine–phosphorylated substrate identified in an early study was caveolin-1 (Cav1), the caveolae coat protein (Glenney, 1989; Parton and del Pozo, 2013). Y14-phosphorylated Cav1 (pY14Cav1) stabilizes focal adhesion components promoting Src- and ROCK-dependent focal adhesion turnover, cell migration, and tumor metastasis (Grande-Garcia *et al.*, 2007; Goetz *et al.*, 2008a; Joshi *et al.*, 2008; Nethe *et al.*, 2010; Boscher and Nabi, 2013; Ortiz *et al.*, 2016). Here we show that increased vinculin tension in focal adhesions is associated with pY14Cav1 stimulation of prostate cancer cell migration.

Cav1 contains a highly conserved caveolin scaffolding domain (CSD; amino acids 82–101), including the essential F92TVT95 segment, which mediates Cav1 interaction with multiple signaling molecules, such as Src family tyrosine kinases, growth factor receptors, endothelial nitric oxide synthase (eNOS), and G proteins (Li *et al.*, 1995, 1996; Couet *et al.*, 1997; Garcia-Cardena *et al.*, 1997; Nystrom *et al.*, 1999; Hoop *et al.*, 2012). The CSD is also required for Cav1 regulation of integrin-dependent endocytosis, indicating a potential role for the CSD in integrin-dependent cell adhesion and migration (Hoffmann *et al.*, 2010). A cell-permeable peptide sequence from antennapedia (AP) fused to the CSD sequence (amino acids 82–101 of Cav1), namely AP-Cav, mimics CSD function, inhibiting eNOS and blocking nitric oxide release from endothelial cells in vitro (Bucci *et al.*, 2000; Gratton *et al.*, 2003; Bernatchez *et al.*, 2005). AP-Cav inhibition of eNOS decreases vasodilation, inflammation, and hyperpermeability of tumor microvasculature, thereby blocking tumor angiogenesis and delaying tumor progression in vivo (Bucci *et al.*, 2000; Gratton *et al.*, 2003; Bernatchez *et al.*, 2005). This suggests that the CSD-mimicking peptides might represent an effective anticancer therapy (Williams and Lisanti, 2005). However, whether AP-Cav peptide also affects promigratory functions of pY14Cav1 in tumor cells is not known.

Cav1 Y14 phosphorylation induces conformational changes that spatially separate Cav1 molecules within the Cav1 oligomer and has been predicted to alter the conformation and/or accessibility of the CSD, facilitating CSD interaction with other proteins (Shajahan *et al.*, 2012; Zimnicka *et al.*, 2016). Indeed, Y14 phosphorylation of Cav1 increases eNOS binding, an interaction mapped to a 10–amino acid sequence within the CSD (Chen *et al.*, 2012; Trane *et al.*, 2014). We show here that phosphomimetic Y14D Cav1 mutation enhances Cav1 binding to focal adhesion proteins. Further, pY14Cav1 stabilization of focal adhesion proteins, promotion of vinculin tension, and cell migration require an intact CSD and are inhibited by AP-Cav peptides. These studies identify pCav1 as a molecular regulator of focal adhesion tension and define a novel role for the CSD in promigratory pY14Cav1 function in tumor cells.

RESULTS

The CSD mediates pY14Cav1-dependent FAK stabilization in focal adhesions and cell migration

DU145 prostate cancer cells express Cav1 and caveolae but no detectable pY14Cav1 (Joshi *et al.*, 2008; Gould *et al.*, 2010). Transient expression of Cav1wt and phosphomimetic Cav1Y14D promotes Src/ROCK-dependent FAK stabilization and cell migration of DU145 cells (Joshi *et al.*, 2008), making these cells an excellent model to selectively study the contribution of pY14Cav1. To determine the role of the CSD in pY14Cav1-dependent FAK stabilization in focal adhesions and cell migration, we introduced F92A/V94A mutations (Li *et al.*, 1996; Nystrom *et al.*, 1999; Lajoie *et al.*, 2007) into a wild-type, Y14F dominant-negative mutant and Y14D phosphomimetic mutant of C-terminal Myc– and monomeric red fluorescent protein (mRFP)–tagged Cav1 (Figure 1A). Stable transfection of these Cav1 constructs in DU145 cells resulted in detection by immunoblotting of a higher–molecular weight band corresponding to recombinant Cav1 in addition to endogenous Cav1 (Figure 1B). Antibody against pY14Cav1 selectively detected recombinant Cav1–myc-mRFP in Cav1wt-expressing cells (Figure 1B). Expression of all constructs was reduced relative to endogenous Cav1, and introduction of the F92A/V94A mutation further reduced expression levels (Figure 1B). By confocal microscopy, all constructs were expressed and exhibited the typical cell surface distribution of wild-type Cav1 (Supplemental Figure S1).

To measure FAK stabilization in focal adhesions, we applied fluorescence recovery after photobleaching (FRAP) to peripheral FAK–enhanced green fluorescent protein (EGFP) in focal adhesions of the DU145 Cav1 stable transfectants (Goetz *et al.*, 2008a; Meng *et al.*, 2015). In contrast to Cav1wt and the Cav1Y14D mutant, and similar to Cav1Y14F, the F92A/V94A CSD mutants of Cav1 were unable to stabilize FAK within focal adhesions (Figure 1, C and D). To ensure that differential stable expression levels of the Cav1 mutants (Figure 1B) did not affect the FRAP data, we transiently transfected DU145 cells with the Cav1-mRFP constructs together with FAK-EGFP and selectively analyzed cells expressing similar levels of mRFP. As for the stable transfectants, the F92A/V94A CSD mutants of Cav1 prevented Cav1wt and Cav1Y14D stabilization of FAK in focal adhesions (Supplemental Figure S2). Transwell cell migration assays showed that migration was reduced by stable expression of the F92/V94A CSD and Y14F Cav1 mutants and increased by expression of Cav1Y14D (Figure 1E).

We then treated the DU145 Cav1 stable transfectants with 10 μM control AP or AP-Cav peptides for 6 h and monitored the mobile fraction of focal adhesion–associated FAK-EGFP by FRAP. AP-Cav, but not AP, decreased FAK stabilization in focal adhesions induced by both Cav1wt and Cav1Y14D (Figure 2A). In contrast, only DU145-Cav1wt cells, and not DU145-Cav1Y14D cells, showed decreased FAK stabilization in focal adhesions in response to PP2 inhibition of Src kinase (Figure 2B). Consistently, AP-Cav selectively reduced the migratory ability of all of the DU145 transfectants to the level of the DU145-Cav1Y14F cells without affecting cell viability (Figure 2, C and D). The CSD therefore mediates focal adhesion FAK stabilization and cell motility stimulation due to pY14Cav1.

pY14Cav1 interaction with vinculin

To study the effect of Y14 phosphorylation on Cav1 interaction with its binding partners, and in particular focal adhesion proteins, we constructed glutathione *S*-transferase (GST)–conjugated Cav1 peptides from amino acids 1–101, including both the Y14 phosphorylation site and the CSD. GST pull downs from DU145 whole-cell lysates were analyzed by quantitative mass spectrometry (Figure 3A). Consistent with reports of Cav1–integrin interaction (Wary *et al.*, 1998; del Pozo *et al.*, 2005; Salanueva *et al.*, 2007), integrin β1 was detected but did not show preferred binding to GST-Cav1(1-101) Y14D or Y14F (Y14F/Y14D ratio 0.432, SD 0.281, $p = 0.1718$, $n = 3$). The other focal adhesion proteins detected (vinculin, α-actinin-4, talin-1, and filamin-A/B) all showed significantly preferred binding to GST-Cav1(1-101)Y14D compared with Y14F with vinculin, showing the most robust binding preference to GST-Cav1(1-101)Y14D (Y14F/Y14D ratio 0.150, SD 0.023, $p = 0.0090$, $n = 2$). Supporting its preferred interaction with Cav1Y14D in our proteomic analysis,

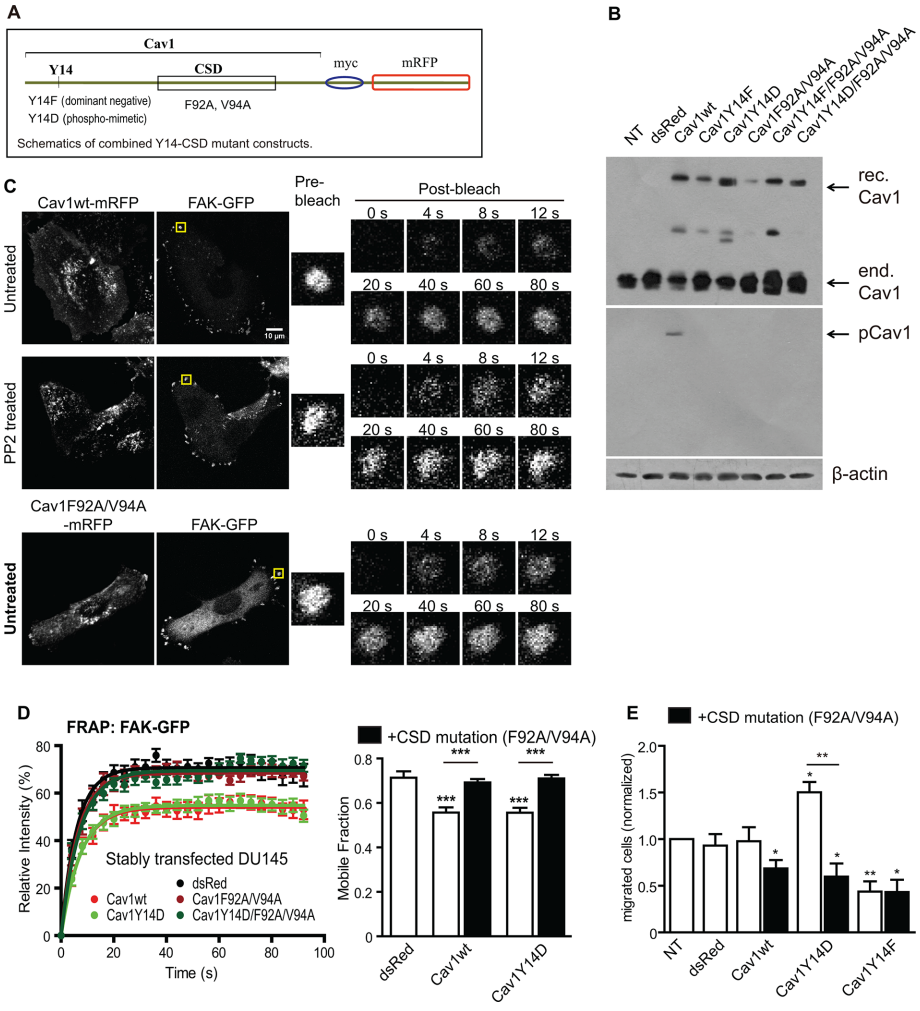

FIGURE 1: CSD mutation prevents pY14Cav1 stabilization of FAK in focal adhesions and cell migration. (A) Schematics showing the combined Cav1 Y14-CSD mutant constructs. (B) Western blot of Cav1 and pY14Cav1 in DU145 and stably transfected DU145 cells (rec., recombinant; end., endogenous.) (C) Representative FRAP images of DU145-Cav1wt (untreated and PP2 treated) and DU145-Cav1F92A/V94A cells transiently transfected with FAK-EGFP. (D) Bar graphs of intensity recovery curves and mobile fraction of FAK-EGFP in focal adhesions of stably transfected DU145 cell lines. Data represent mean ± SEM from one of three independent experiments ($n > 8$ for each cell line). One-way analysis of variance (ANOVA) with Tukey posttest; ***$p < 0.001$. (E) Bar graph of the number of migrated DU145 and stably transfected DU145 cells (normalized to nontransfected DU145 cells) in Transwell migration assays ($n = 5$; two-tailed unpaired t test; *$p < 0.05$; **$p < 0.01$).

coimmunoprecipitation of filamin A with Cav1 is Src-dependent (Sverdlov *et al.*, 2009). Western blotting of GST pull downs confirmed the preferential binding of vinculin to GST-Cav1Y14D compared with GST and GST-Cav1Y14F (Figure 3B). As for FAK, vinculin-Venus showed increased stabilization in focal adhesions of Cav1wt and Cav1Y14D DU145 cells but not in cells expressing F92A/V94A or Y14F Cav1 mutants (Figure 3C). pY14Cav1 therefore interacts with and regulates vinculin stabilization in focal adhesions in a CSD-dependent manner.

CSD-dependent pY14Cav1 regulation of vinculin tension

On the basis of the enriched binding of vinculin to GST-Cav1Y14D and increased vinculin tension at leading-edge focal adhesions (Grashoff *et al.*, 2010), we expressed vinculin tension sensors together with myc-tagged Cav1 mutants in DU145 cells to examine pY14Cav1 regulation of vinculin tension in focal adhesions. FRET efficiency of tension sensor (VinTS) and control tail-less (VinTL) constructs of vinculin was tested by acceptor photobleaching. As shown in Figure 4, A and B, VinTL showed constant high FRET efficiency, equivalent to that of VinTS in control or Cav1Y14F-transfected DU145 cells. VinTS, but not VinTL, displayed lower FRET efficiency in Cav1wt-myc– and Cav1Y14D-myc–transfected DU145 cells, suggesting that pY14Cav1 increases vinculin tension in focal adhesions.

We then used prostate cancer cell lines that differentially express Cav1 and pY14Cav1 to test the role of endogenous Cav1 in vinculin tension. LNCaP cells do not express Cav1, DU145 cells express Cav1 but not pY14Cav1, and only PC3 cells express pY14Cav1 (Joshi *et al.*, 2008; Gould *et al.*, 2010). PC3 showed significantly more vinculin tension (less FRET efficiency) than DU145 and LNCaP cells (Figure 4C, D). Blocking F-actin remodeling (ROCK inhibitor Y27632) and actin polymerization (latrunculin A [LatA]) relieved vinculin tension (high FRET efficiency) in PC3 cells, whereas stabilization of actin filaments with jasplakinolide (Jasp) induced high vinculin tension (low FRET efficiency) in LNCaP and DU145 cells (Figure 4, C and D). In PC3 cells, vinculin tension was decreased by PP2 treatment and Cav1 knockdown, and therefore was both Cav1 and Src dependent (Figure 5A). Similarly, PP2 prevented vinculin tension in Cav1wt-expressing DU145 cells (Figure 5B). The ability of PP2 to prevent vinculin tension in Cav1Y14D cells (Figure 5B) contrasts with the inability of Src inhibition to reverse Cav1Y14D-dependent FAK stabilization (Figure 2B). Src-dependent Y14 phosphorylation of Cav1 therefore appears to be sufficient for the stabilization of focal adhesion components, but additional Src activity is required for vinculin tension.

pCav1-dependent vinculin tension in PC3 cells is disrupted by treatment with AP-Cav peptide but not control AP peptide; in LNCaP and DU145 cells lacking pCav1, vinculin tension levels are not affected by either AP or AP-Cav treatment (Figure 5C). Further, both F92A/V94A mutation and AP-Cav peptide treatment reversed increased vinculin tension in Cav1wt- and Cav1Y14D-expressing DU145 cells (Figure 5, D and E). These data support a role for the CSD in regulating pY14Cav1-dependent vinculin tension at focal adhesions.

The dramatic differences in average vinculin tension in response to the various conditions led us to analyze vinculin FRET data of individual focal adhesions by binning each focal adhesion in small intervals of FRET efficiency values (FRET interval 0.04; range 0–0.8). As shown in Figure 6A, focal adhesions with intermediate FRET values (0.12–0.24) were present in both Jasp- and LatA-treated cells. However, focal adhesions with FRET values below this intermediate range were present only in Jasp-treated cells and with FRET values above this range only in LatA-treated cells. On the basis of this, we defined individual focal adhesions as high tension (FRET 0–0.12),

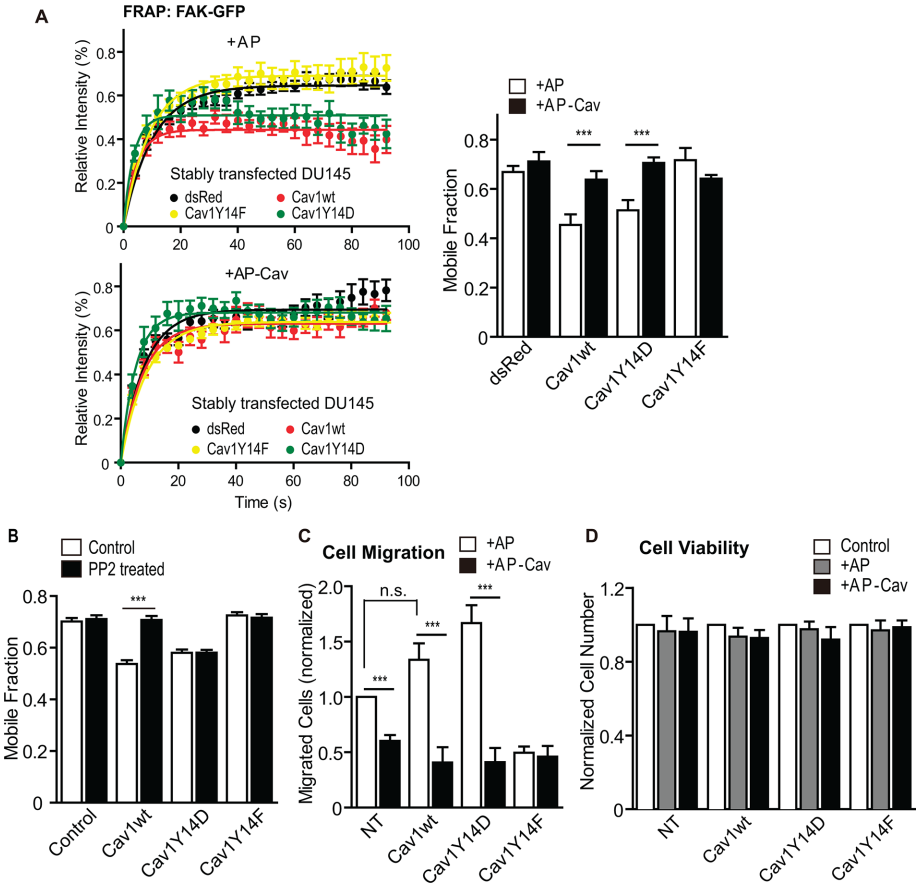

FIGURE 2: The CSD-mimicking peptide AP-Cav decreases pY14Cav1-dependent FAK stabilization in focal adhesions and cell migration. (A) Intensity recovery curves and mobile fraction for FAK-EGFP in focal adhesions from FRAP assays of the stable DU145 Cav1 transfectants treated with AP or AP-Cav peptide for 6 h. Data represent mean ± SEM from one of three independent experiments ($n > 8$ for each cell line). Two-tailed unpaired t test; ***$p < 0.001$. (B) Mobile fraction of FAK-EGFP in focal adhesions of DU145 (NT) and stably transfected DU145 cell lines (Cav1 constructs as indicated) untreated or PP2 treated (control: DU145 cells transfected with FAK-EGFP only). Bar graph represents mean ± SEM of three independent experiments ($n > 10$ for each cell type/treatment for each experiment). One-way ANOVA with Tukey posttest; ***$p < 0.001$. (C) Quantification of migrated cell numbers in Transwell migration assays of DU145 (NT) and stably transfected DU145 cells (Cav1 constructs as indicated) treated with AP or AP-Cav for 6 h ($n = 5$). Two-tailed unpaired t test; ***$p < 0.001$. (D) Quantification of adherent cells after treatment with AP or AP-Cav for 6 h as a measure of cell viability of nontransfected DU145 (NT) and stable DU145 Cav1 transfectants as indicated. The numbers of cells were normalized to that of untreated cells. No significant difference was detected with one-way ANOVA with Tukey posttest ($n = 5$).

medium tension (FRET 0.12–0.24), and low tension (FRET 0.24–0.8) based on their FRET values (Figure 6A). In PC3 cells, as observed for LatA, Y27632, PP2 treatment, siCav1 knockdown, and AP-Cav decreased high-tension focal adhesions and increased low-tension focal adhesions (Figure 6B). Consistently in DU145 cells, overexpression of Cav1wt and Cav1Y14D, but not Cav1Y14F, increased high-tension focal adhesions, an increase that could be reversed by CSD mutation, AP-Cav treatment, and PP2 treatment (Figure 6, C and D). This suggests that CSD- and Src-dependent pY14Cav1 shifts the tension distribution of cellular focal adhesions, enhancing or stabilizing those focal adhesions with higher tension.

pY14Cav1 stabilizes vinculin tension in focal adhesions

We then analyzed vinculin tension using FRET-sensitized emission (FRET SE) analysis over ~6.5 min at a high frame rate (~2 s/frame) in live cells. Representative traces of single focal adhesions of PC3 cells show a high degree of fluctuation in FRET values over time. Treatment with LatA or Y27632 dramatically increased the range of FRET values observed in individual focal adhesions over time (Figure 7A). Analysis of multiple focal adhesions showed that average FRET values and the SD increased significantly on release of focal adhesion tension with LatA and Y27632. Consistent with the fixed cell FRET data (Figure 6), plotting the average FRET value for individual focal adhesions for each condition showed that average FRET values could be binned into high, medium, and low values, with actin depolymerization (LatA) and ROCK inhibition (Y27632) associated with a shift from high- to low-tension focal adhesions (Figure 7A). Similarly, FRET average and SD increased significantly on siCav1 knockdown, PP2 inhibition of Src, and AP-Cav treatment, which were also associated with a shift from high- to low-tension focal adhesions (Figure 7B).

We then plotted the FRET value ranges (over 6.5 min) for individual focal adhesions and color coded focal adhesion tension ranges of individual cells (Figure 8A). In the more motile PC3 cells, as well as in controls (siCtl- or AP-treated PC3 cells), FRET ranges were lower and narrower and consistent both between different cells and among focal adhesions within the same cell (Figure 8A). Consistent with our analysis of individual focal adhesions (Figure 7B), inhibiting motility by targeting Cav1 with siCav1, PP2, or AP-Cav was associated with increased tension ranges for individual focal adhesions and increased variation between the FRET ranges observed for individual cells (Figure 8A). Of interest, FRET ranges were highly similar between focal adhesions of an individual cell, irrespective of the FRET average or FRET range. This is reflected in the significant increase in average cellular FRET (average FRET of all focal adhesions per cell) but not in SD of average focal adhesion FRET per cell in PP2-, siCav1-, and AP-Cav–treated cells (Figure 8B). pCav1 promotion of tumor cell motility is therefore associated with CSD-dependent dampening of the range of vinculin tension in cellular focal adhesions, thereby maintaining cellular focal adhesions at high tension.

DISCUSSION

Functional interaction between Y14 phosphorylation and the CSD controls promigratory Cav1 activity

Cav1 is a 178–amino acid integral membrane protein whose highly conserved CSD binds and regulates the activity of multiple receptors, scaffold proteins, and kinases (Okamoto *et al.*, 1998; Goetz *et al.*, 2008b). Cav1 is also a major Src kinase substrate (on tyrosine 14), and pCav1 promotes pseudopodial protrusion, RhoA activation, focal adhesion dynamics, and the migration and invasion of

A

Gene ID	Protein name	N	average # peptides	Binding ratio Cav1Y14F/Cav1 Y14D		
				Mean	SD	P value
P18206-2	Isoform 1 of Vinculin	2	3	0.150	0.023	0.0090
Q5TCU6	Talin 1	3	13	0.257	0.038	0.0260
O43707	Alpha-actinin-4	3	29	0.271	0.015	0.0230
Q5HY54	Filamin-A	5	33	0.289	0.033	0.0090
O75369-2	Isoform 2 of Filamin-B	4	45	0.311	0.040	0.0280
P05556-2	Isoform Beta-1B of Integrin beta-1	3	5	0.432	0.281	0.1718

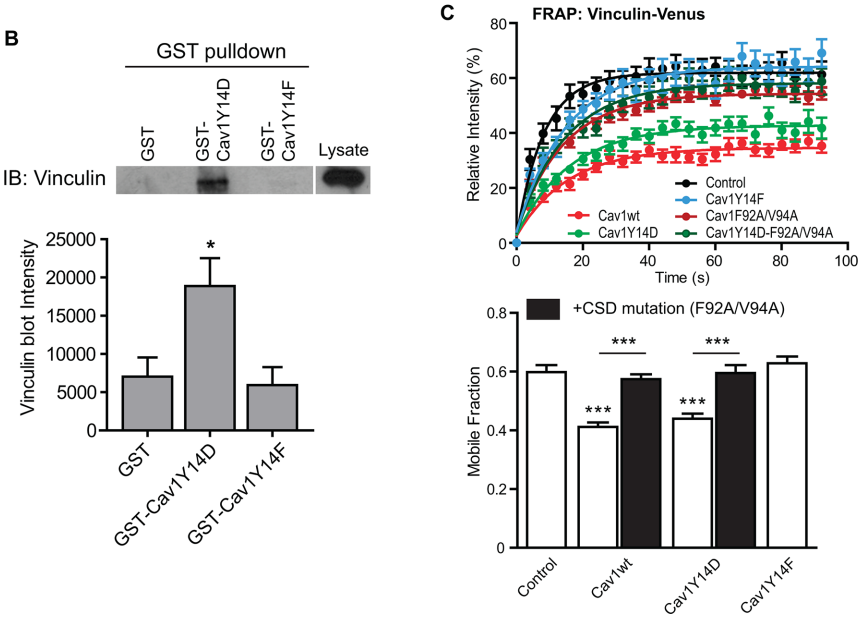

FIGURE 3: pY14Cav1 interacts with vinculin and regulates its stability within focal adhesions. (A) Focal adhesion proteins detected by quantitative proteomics analysis of GST-Cav1Y14D and GST-Cav1Y14F pull-down elution. Data represent six independent experiments. *N*, number of experiment repeats that detect the same protein; "average # peptides" indicates the average number of peptides detected that match the protein; "binding ratio Cav1Y14F/Cav1Y14D" indicates the ratio of the quantity of the binding partner detected from the elution from GST-Cav1Y14F vs. that from GST-Cav1Y14D. (B) Western blot of elution from GST pull down labeled with an anti-vinculin antibody, showing the preferential binding of vinculin with GST-Cav1Y14D. Blots were quantified with the intensity of the vinculin blots, and the bar graph represents mean ± SEM of six independent experiments. One-way ANOVA with Tukey posttest; *$p < 0.05$ compared with both of the others. (C) Intensity recovery curve and mobile fraction of FRAP assays on vinculin-Venus within focal adhesions of nontransfected DU145 (NT) and stable DU145 Cav1 transfectants as indicated. Intensity recovery curves represent one of three independent experiments; mobile fraction bar graph represents mean ± SEM of three independent experiments ($n > 12$ for each cell line for each experiment). One-way ANOVA with Tukey posttest; ***$p < 0.001$.

metastatic cancer cells (Parat *et al.*, 2003; Gaus *et al.*, 2006; Grande-Garcia *et al.*, 2007; Goetz *et al.*, 2008a; Joshi *et al.*, 2008; Nethe *et al.*, 2010; Boscher and Nabi, 2013; Ortiz *et al.*, 2016). We demonstrate here that pCav1 control of focal adhesion dynamics and tumor cell migration is CSD-dependent and mediated through enhanced interaction of pCav1 with multiple focal adhesion proteins and increased tension of vinculin in focal adhesions. Src-dependent control of CSD binding affinity for focal adhesion proteins through Y14 phosphorylation therefore controls focal adhesion tension and thereby tumor cell migration.

Early studies showing pCav1 localization to focal adhesions (Lee *et al.*, 2000; Beardsley *et al.*, 2005) were challenged because the monoclonal anti-pY14Cav1 antibody was shown to cross-react with phospho-paxillin (Hill *et al.*, 2007). Nevertheless, numerous studies have shown functional roles for Cav1, and more specifically pCav1, using Y14D and Y14F Cav1 phosphomimetics and Src inhibition, in focal adhesion signaling, organization, and dynamics, integrin trafficking, and cell migration (Beardsley *et al.*, 2005; del Pozo *et al.*, 2005; Gaus *et al.*, 2006; Grande-Garcia *et al.*, 2007; Goetz *et al.*, 2008a; Joshi *et al.*, 2008; Nethe *et al.*, 2010; Ortiz *et al.*, 2016). Indeed, Rac1 activation has been shown to promote the association of Cav1 with peripheral focal adhesions (Nethe *et al.*, 2010). Increased interaction of GST-Cav1Y14D with multiple focal adhesion proteins relative to GST-Cav1Y14F (Figure 3B) argues that pCav1 interacts with and is in proximity to focal adhesion proteins, although whether these interactions are direct or not remains to be determined.

Numerous studies have reported protein interactions for the CSD; functional roles for this highly conserved domain have been described using CSD mutants, such as the F92A/V94A Cav1 mutation used in this study, and membrane-traversing CSD peptides (cavtratin or AP-Cav; Nystrom *et al.*, 1999; Gratton *et al.*, 2003; Bernatchez *et al.*, 2005). However, close proximity of the CSD to the cell membrane and consequent low accessibility to binding partners has led to reassessment of the functionality of the CSD domain (Byrne *et al.*, 2012; Collins *et al.*, 2012; Ariotti *et al.*, 2015). Cav1 Y14 phosphorylation induces conformational changes that increase the spacing between Cav1 molecules (Shajahan *et al.*, 2012; Zimnicka *et al.*, 2016). Indeed, Cav1 Y14 phosphorylation has been shown to enhance CSD interaction with eNOS (Chen *et al.*, 2012). Y14 phosphorylation induced conformational changes may thereby distance the CSD from the membrane, promoting CSD accessibility to binding partners, including the focal adhesion proteins reported here.

A scaffolding function for pY14Cav1 at focal adhesions is supported by the requirement for the CSD in the regulation of pY-14Cav1 activity in focal adhesions and tumor cell migration (Figure 2). Disruption of pY14Cav1-dependent focal adhesion stabilization, vinculin tension, and cell migration by the membrane-permeable, CSD-mimicking peptide AP-Cav defines a critical role for the CSD in focal adhesion dynamics and migration of tumor cells. The AP-Cav peptide inhibits angiogenesis and delays tumor progression in vivo (Bucci *et al.*, 2000; Gratton *et al.*, 2003) such that CSD-mimicking peptides may represent an effective anticancer therapy (Williams and Lisanti, 2005). Our data suggest that therapeutic use of CSD-mimicking peptides may also affect pY14Cav1-dependent tumor cell migration, enhancing the potential value of these CSD-targeted reagents as anticancer therapeutics.

pCav1 promotes vinculin tension at focal adhesions

pY14Cav1 stabilizes FAK in focal adhesions, which is associated with FAK-Y397 phosphorylation and focal adhesion disassembly and cell migration (Hamadi *et al.*, 2005; Goetz *et al.*, 2008a; Joshi *et al.*, 2008). Vinculin is also activated by Src phosphorylation of Y1065 and stabilizes various components of focal adhesions, including

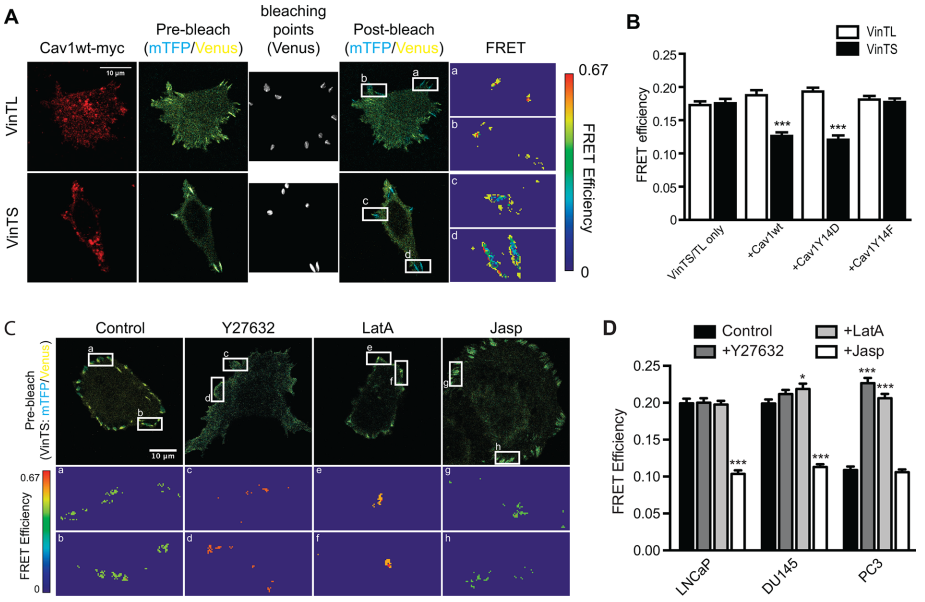

FIGURE 4: Use of a FRET sensor to report on vinculin tension in metastatic prostate cancer cells. (A) Representative images of acceptor photobleaching FRET assay on vinculin tension sensor (VinTS) and control vinculin tailless (VinTL) in DU145 cells cotransfected with Cav1wt-myc. Cells were fixed and Cav1-myc constructs detected by immunolabeling with anti-myc tag antibody. Insets, enlarged focal adhesions color-coded for FRET efficiency. Scale bar, 10 µm. (B) Quantification of FRET efficiency of VinTS or VinTL of indicated DU145 Cav1 transfectants. (C) Representative images of prebleach and FRET efficiency of PC3 cells, untreated (Control) cells, or cells treated with Y27632, LatA, or Jasp. (D) Quantification of VinTS FRET efficiency in focal adhesions of LNCaP, DU145, and PC3 cells, untreated (Control) cells, or cells treated with Y27632, LatA, or Jasp as indicated. For B and D, data represent mean ± SEM of three independent experiments ($n > 20$ for each cell type/treatment for each experiment). One-way ANOVA with Tukey posttest for B and two-way ANOVA with Dunnett posttest for D; *$p < 0.05$; ***$p < 0.001$.

FAK, in a force-dependent manner (Carisey *et al.*, 2013). Indeed, PP2 disrupts the Src-dependent activation of vinculin and tension development in airway smooth muscle cells (Zhang *et al.*, 2004; Huang *et al.*, 2014). We show here that pCav1 also stabilizes vinculin and regulates vinculin tension in focal adhesions. Curiously, whereas FAK stabilization in focal adhesions by Cav1Y14D is insensitive to Src inhibition (Figure 2B), increased vinculin tension induced by Cav1Y14D remains PP2 sensitive (Figure 5B). This suggests that Src-dependent Cav1 Y14 phosphorylation is sufficient to stabilize focal adhesion components but not to induce vinculin tension. pCav1 stabilization of focal adhesion components may enable the Src phosphorylation of vinculin Y1065 required for its conformation-based activation and tension (Zhang *et al.*, 2004; Huang *et al.*, 2014).

Further, mechanical tension drives Src-dependent Cav1 Y14 phosphorylation (Radel and Rizzo, 2005; Joshi *et al.*, 2012). At the same time, Cav1 promotes Csk-dependent inactivation of Src and prevents Src/p190RhoGAP inhibition of RhoGTPase signaling, thereby driving cell polarization and motility (Grande-Garcia *et al.*, 2007; Place *et al.*, 2011). The results taken together suggest that Src-dependent pY14Cav1 stabilization of focal adhesion proteins is a central component of a feedback loop that enables temporal vinculin activation, unfolding, and focal adhesion tension.

Our data suggest that pCav1 generally increases vinculin tension in focal adhesions and dampens the elasticity of tension variations in focal adhesions, paralleling the effects of actin cytoskeleton stabilization. Indeed, the effect on focal adhesion vinculin tension observed on modulation of the actin cytoskeleton (LatA, Y27632, Jas) was highly similar to that induced by altering pCav1 status and function (Figures 6 and 7). This can be seen in the higher abundance of high-tension focal adhesions in pCav1-expressing and Jasp-treated cells (Figure 6) and in the larger FRET range of individual focal adhesions over time in PC3 cells treated with siCav1, PP2, LatA, or Y27632 (Figure 7B). This suggests that pCav1 is a molecular effector that promotes actin- and ROCK-dependent focal adhesion tension. Consistently, pCav1 induces RhoA activation and promotes Rho/ROCK-dependent cell migration and invasion (Grande-Garcia *et al.*, 2007; Joshi *et al.*, 2008).

pCav1-dependent vinculin tension and tumor cell migration

Vinculin interacts with both the talin-integrin complex and the actin cytoskeleton and is therefore closely involved in focal adhesion tension-induced signaling (Cohen *et al.*, 2006; Ziegler *et al.*, 2006; del Rio *et al.*, 2009; Kanchanawong *et al.*, 2010). A constitutively active vinculin mutant shows less turnover from focal adhesions and leads to enlarged focal adhesions in a high-tension environment (Balaban *et al.*, 2001; Cohen *et al.*, 2006; Humphries *et al.*, 2007). Tension maintains vinculin in focal adhesions, and a mutated active vinculin activates integrins and stabilizes other focal adhesion proteins within focal adhesions (Carisey *et al.*, 2013). A more recent study found a plastic relationship between vinculin tension and the size and lifetime of focal adhesions and identified a subpopulation of adhesions with stable vinculin tension (Hernandez-Varas *et al.*, 2015). These data are consistent with our identification of a population of focal adhesions that maintain a midrange tension irrespective of modulation of pCav1 status or actin polymerization state.

The large fluctuations that we observe in vinculin tension over time were reported previously for both vinculin and talin (Margadant *et al.*, 2011; Plotnikov *et al.*, 2012; Hernandez-Varas *et al.*, 2015) and were predicted by modeling of a molecular clutch linking the actin cytoskeleton to the substrate (Chan and Odde, 2008). Vinculin is required to couple retrograde flow to focal adhesions and for ROCK-dependent focal adhesion traction in response to ECM rigidity (Plotnikov *et al.*, 2012; Thievessen *et al.*, 2013). The molecular clutch hypothesis argues that linking the ECM to the actin cytoskeleton through integrins and focal adhesions engages and directs retrograde actin flow to drive lamellipodial protrusion (Mitchison and Kirschner, 1988). Slippage between retrograde flow and substrate will reduce force transmission and tension at focal adhesions and thereby lamellipod protrusion and cell motility (Case and Waterman, 2015). By dampening force fluctuation in focal adhesions, pCav1 may promote clutch engagement, driving membrane protrusion and migration of the cancer cells studied here.

Consistent with this interpretation, focal adhesions of pCav1 expressing PC3 cells show a general shift to high-tension FRET ranges. pCav1 disruption with PP2, siCav1, or AP-Cav resulted in reduced average vinculin tension values for cellular focal adhesions and larger tension ranges, indicative of increased slippage between

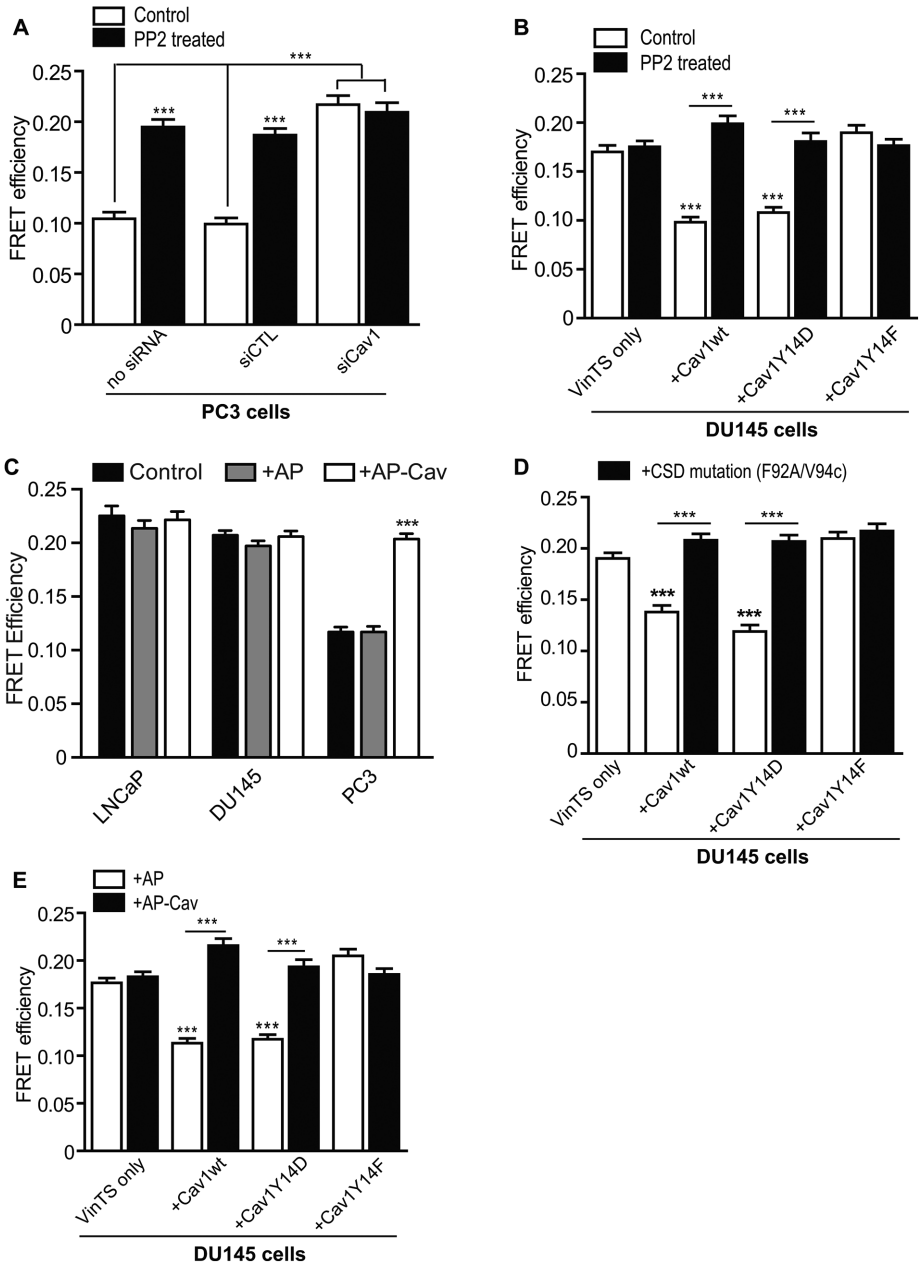

FIGURE 5: pY14Cav1 induces vinculin tension in a CSD-dependent manner. (A) Quantification of FRET efficiency of VinTS in focal adhesions of siRNA-transfected PC3 cells (no siRNA, siCTL, or siCav1) and/or PP2 treatment. (B) Quantification of FRET efficiency of VinTS of DU145 Cav1 transfectants as indicated, untreated (control) or treated with PP2. (C) Quantification of VinTS FRET efficiency in focal adhesions of LNCaP, DU145, and PC3 cells, untreated (Control) cells, or cells treated with AP/AP-Cav as indicated. (D, E) Quantification of FRET efficiency of VinTS of variously transfected DU145 cells as indicated, untreated (D) or treated with AP/AP-Cav for 6 h (E). Data represent mean ± SEM of three independent experiments (n >20 for each cell type/treatment for each experiment). One-way ANOVA with Tukey posttest; ***p < 0.001.

actin flow and substrate adhesions. Although not directly addressed in this study, our data do not preclude a leading edge/trailing edge gradient for vinculin tension (Grashoff *et al.*, 2010). Indeed, pCav1 association with the leading edge (Nomura and Fujimoto, 1999; Parat *et al.*, 2003; Joshi *et al.*, 2008) suggests that it acts predominantly at protrusive actin regions. Our data instead argue that pCav1 expression generally maintains cellular focal adhesions at high tension, that is, shifts cells to high gear.

Cav1 expression is closely associated with a poor prognosis in prostate and other cancers, including breast cancer (Yang *et al.*, 1999; Satoh *et al.*, 2003; Sloan *et al.*, 2009; El-Gendi *et al.*, 2012). Collagen density and extracellular matrix organization are associated with tumorigenesis (Ursin *et al.*, 2005; Provenzano *et al.*, 2006). Increasing matrix stiffness links to cellular tension to promote tumor migration and metastasis through focal adhesion signaling (Paszek *et al.*, 2005; Levental *et al.*, 2009; Kraning-Rush *et al.*, 2012). Fluctuations in focal adhesion tension sample ECM rigidity and guide cellular migration to areas of ECM stiffness (Plotnikov *et al.*, 2012). The extent to which pCav1 induction of cellular focal adhesion tension mediates the cancer cell response to matrix stiffness and is involved in Cav1 function in cancer progression remains to be determined. However, inasmuch as Cav1 responds to mechanical stress (Radel and Rizzo, 2005; Joshi *et al.*, 2012), is a key component of caveolae that protect against mechanical induced damage of the plasma membrane (Sinha *et al.*, 2010), promotes Rho/ROCK-dependent cell migration (Joshi *et al.*, 2008), and, as shown here, regulates focal adhesion tension, Cav1 is critically placed to contribute to and mediate the tumor cell response to mechanical stress and ECM stiffness.

MATERIALS AND METHODS

Antibodies and reagents

Bovine serum albumin solution (BSA; 30%), and mouse anti–β-actin antibodies were purchased from Sigma-Aldrich. Rabbit anti-Cav1 and rabbit anti-FAK were purchased from Santa Cruz Biotechnology, and rabbit anti-pY14Cav1 and rabbit anti-Cav antibodies from Transduction Laboratories. Horseradish peroxidase (HRP)–conjugated mouse and rabbit secondary antibodies were purchased from Jackson ImmunoResearch Laboratories. Phalloidin and secondary antibodies conjugated to Alexa 488, 568, or 647 were purchased from Life Technologies, Invitrogen. PP2 and Y27632 were purchased from EMD Millipore. LatA and Jasp were purchased from Sigma-Aldrich. AP and AP-Cav were as described (Bernatchez *et al.*, 2005).

Plasmids

C-terminal–tagged, myc/mRFP-tagged Cav1wt, Cav1Y14F, Cav1Y14D, and Cav1Y14R under control of the cytomegalovirus promoter in pcDNA3 plasmid were as previously described (Goetz *et al.*, 2008a; Joshi *et al.*, 2008). The Cav1 scaffolding domain mutant (Cav1F92A/V94A) and the combined mutants (Cav1Y14F/F92A/V94A and Cav1Y14D/F92A/V94A) were generated using the following sets of primers: for F92A/V94A-F,

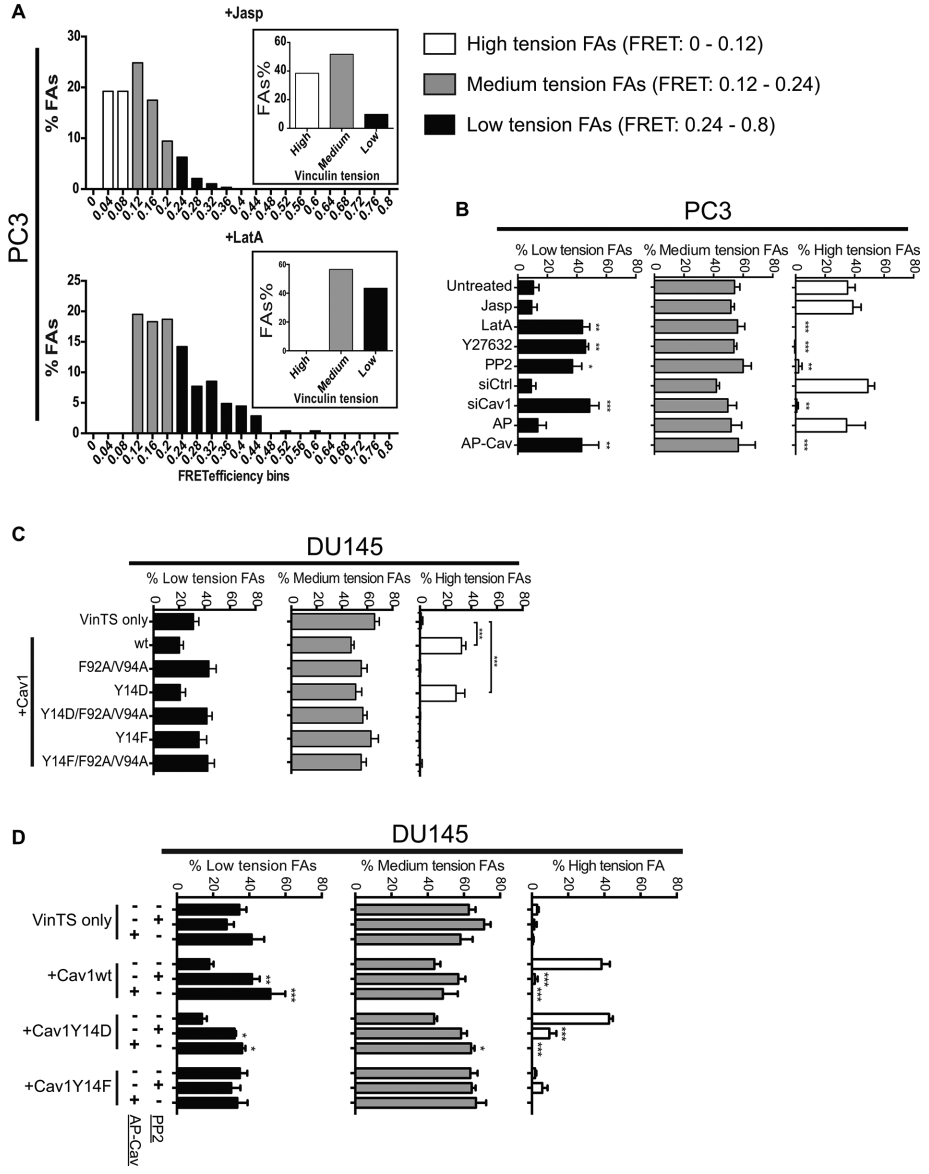

FIGURE 6: pY14Cav1 shifts the vinculin tension distribution of focal adhesions. (A) FRET AB measurements of vinculin tension of focal adhesions of PC3 cells treated with Jasp and LatA were binned at interval of 0.04 unit. Focal adhesions were arbitrarily divided into groups of high (FRET 0–0.12), medium (FRET 0.12–0.24), and low (FRET 0.24 – 0.8) tension by comparing the Jasp- and LatA-treated cells. (B–D) Percentage of low-/medium-/high-tension focal adhesions in PC3 and DU145 cells with various treatments and transfections as noted. Data represent mean ± SEM of three independent experiments ($n > 20$ for each cell type/treatment for each experiment). One-way ANOVA with Tukey posttest; *$p < 0.05$; **$p < 0.01$; ***$p < 0.001$.

5′cac cac cgc cac tgc gac gaa ata ctg g3′, and for F92A/V94A-R, 5′cca gta ttt cgt cgc agt ggc ggt ggt g3′; for Cav1-*Bam*HI-R, 5′ggg gat ccc tat ttc ttt ctg ca agt tga tgc gga c3′, and for Cav1-*Hin*dIII-F, 5′gga agc tta gca tgt ctg ggg gca aat ac3′; where either Cav1wt or its Y14 mutants were used as templates for postoverlapping extension. The final PCR-amplified products, Cav1F92A/V94A, Cav1Y14F/F92A/V94A, or Cav1Y14D/F92A/V94A, were TA-cloned (Invitrogen), restriction digested (by *Hin*dIII) and sequence verified before subcloning back into pRFP-N1 at *Eco*R1-*Bam*H1 restriction sites. Restriction enzymes (*Eco*R1 and *Bam*H1) were purchased from New England Biolabs. T4 ligase was purchased from Invitrogen.

Cell culture, transfection, and drug treatment

The human DU145 cell line was from the American Type Culture Collection and maintained in complete RPMI 1640 supplemented with 10% fetal bovine serum. Stable DU145 cell lines expressing dsR or the Cav1 constructs were prepared by transfecting dsR or the Cav1 construct expression vectors using Effectene (Qiagen). Neomycin-resistant cells were selected for 15 d against 400 µg/mL Geneticin (Life Technologies, Invitrogen), and resistant colonies were trypsinized and sorted for mRFP positives by fluorescence-activated cell sorting. Pooled mRFP-positive cells were allowed to recover and expanded in complete medium supplemented with Geneticin. All cell lines were passaged at least twice after recovery from frozen stocks before initiation of experiments and maintained in culture for a maximum of 8–10 passages to minimize phenotypic drift.

Transient plasmid transfection was done 24 h after plating of the cells or small interfering RNA (siRNA) transfection, using Lipofectamine 2000 (Life Technologies, Thermo Fisher Scientific) following the manufacturer's protocol. Experiments were performed 24 h after plasmid transfection. To knock down Cav1, cells were cultured in complete medium for 24 h before transfection with specific mouse Cav1 siRNA or control siRNA SMARTpools (mouse siCav1: L-0058415-00; siCONTROLS: D-001210-01; Dharmacon) using Lipofectamine 2000 transfection reagent (Life Technologies, Thermo Fisher Scientific) following the manufacturer's protocol. Where indicated, cells were treated with 10 µM PP2 for 30 min, 20 µM Y27632 for 1 h, 150 nM Jasp for 2 h, and 150 nM LatA for 30 min.

Western blotting

Cell pellets from 80% confluent cultures were washed with cold phosphate-buffered saline (PBS) and resuspended in lysis buffer (20 mM Tris-HCl, pH 7.6, 0.5% NP-40, 250 mM NaCl, 3 mM EDTA, and 3 mM ethylene glycol tetraacetic acid containing freshly added 2 mM dithiothreitol (DTT), 0.5 mM phenylmethylsulfonyl fluoride, 1 mM sodium vanadate, 2.5 mM sodium fluoride, and 1 µM leupeptin) for 30 min at 4°C, and pelleted at 13,000 rpm at 4°C, and the supernatant was collected and stored at –80°C. Equal amounts of proteins were separated on 12% SDS–PAGE, electroblotted onto nitrocellulose (GE Healthcare Life Sciences), probed with indicated antibodies and HRP-conjugated secondary antibodies, and revealed by enhanced chemiluminescence.

Immunofluorescence labeling

Cells were fixed with 3% paraformaldehyde (PFA) for 15 min at room temperature, rinsed with PBS, permeabilized with 0.1%

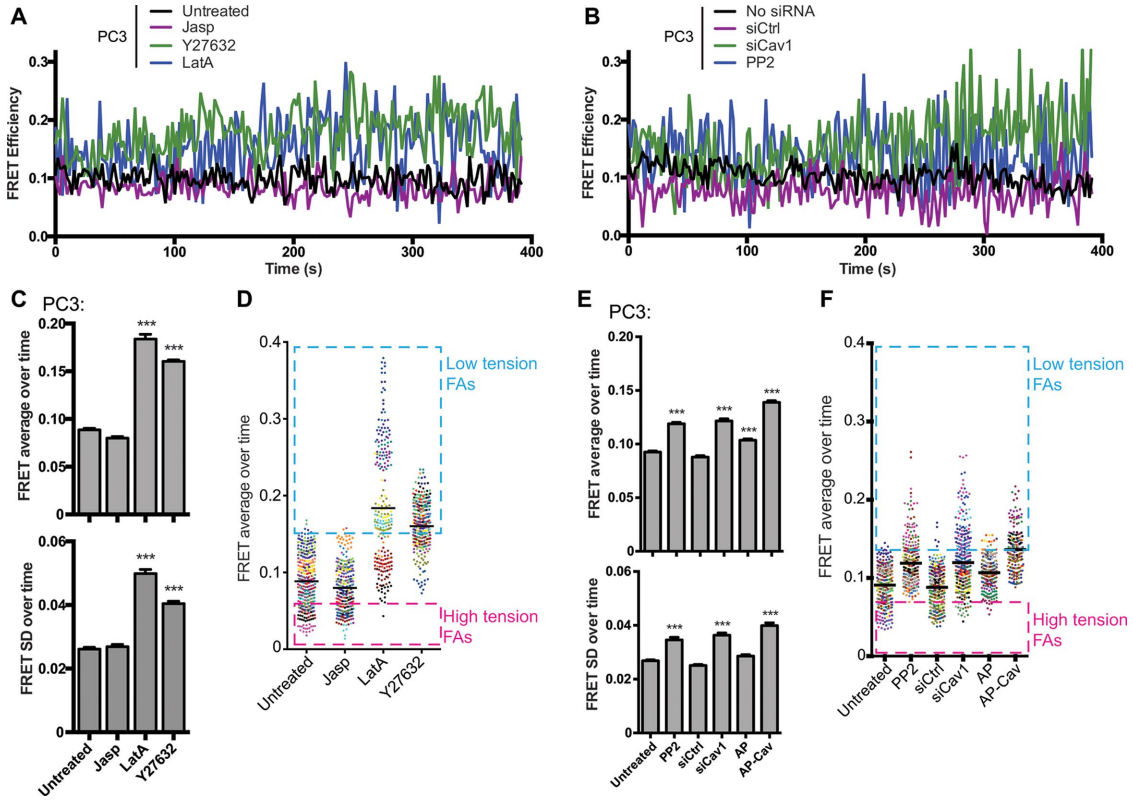

FIGURE 7: Live-cell FRET analysis shows that pY14Cav1 narrows the range of vinculin tension in focal adhesions. PC3 cells transiently transfected with VinTS were treated with Jasp, LatA, or Y27632 (A, C, D) or with PP2, siCtl/siCav1, or AP/AP-Cav (B, E, F) and analyzed by live-cell FRET (sensitized emission, FRET-SE) analysis for ~6.5 min (2-s intervals, 200 frames). Live scans of FRET in individual focal adhesions (A, B), average and SD of FRET values for individual focal adhesions over time (C, E), and a point distribution of individual focal adhesion FRET values (D, F; focal adhesions from the same cell are coded with the same color; line shows average) are shown for the different conditions. Boxes show groupings of high- and low-tension focal adhesions. Data represent mean ± SEM of three independent experiments ($n > 20$ for each cell type/treatment for each experiment). One-way ANOVA with Tukey posttest; ***$p < 0.001$.

Triton X-100 in PBS plus 0.1 mM Ca^{2+} and 1 mM Mg^{2+} (PBS/CM), blocked with PBS/CM containing 2% BSA, and then incubated with primary and fluorescent secondary antibodies in PBS/CM containing 2% BSA. After labeling, the coverslips were mounted in CelVol (Celanese) or Prolong Gold (Life Technologies, Thermo Fisher Scientific), and images were acquired with a 60× or 100× Plan-Apochromat objectives (numerical aperture [NA] 1.35) of an Olympus FV1000 confocal microscope or with a 100× HC PL APO objective (NA 1.40; oil) of a Leica TCS SP8 confocal microscope.

FRAP and FRET analysis

FRAP was performed on an Olympus FV1000 confocal microscope equipped with a 60× Plan Apochromat objective (NA 1.35; oil) and SIM scanner. Cells were plated at low density on fibronectin (FN; 10 µg/ml) for 24 h in an eight-well µ-slide chamber (ibidi) and transfected with denoted plasmid constructs; experiments were performed 24 h later at 37°C in bicarbonate-free medium. PP2 at 10 µM was applied to cells 30 min before imaging. Alternatively, 18 h after transfection, culture medium was replaced with serum-free medium containing 10 µM AP or AP-Cav for 6 h. For each FRAP analysis, a prebleach frame was acquired, followed by a single bleach event, using the simultaneous and independent stimulation of the 405-nm laser line of the SIM scanner. Fluorescence recovery was followed at 4-s time intervals until the intensity reached a plateau. Fluorescence intensity during recovery was normalized to the prebleach intensity. Normalized intensity value of the recovery plateau in each bleached area was calculated as the mobile fraction using Prism 4 (GraphPad). Graphs are representative of a minimum of three independent experiments in which between 10 and 25 focal adhesions were bleached.

FRET was performed on a Leica TCS SP8 confocal microscope with a 100× HC PL APO objective (NA 1.40; oil) or a 63× water immersion objective, using either FRET AB (acceptor bleaching) or FRET SE (sensitized emission) Leica software modules. Cells were plated at low density on FN (10 µg/ml) in an eight-well µ-slide chamber (ibidi) and transfected with the indicated plasmids 24 h postplating. For FRET AB, cells were fixed with 3% PFA 24 h after transfection and then permeabilized with 0.1% Triton X-100, blocked with 2% BSA, and incubated with specific primary antibodies (mouse anti-myc tag or rabbit anti-Cav1) and Alexa Fluor 647–conjugated secondary antibodies. Regions of interest were drawn around visible focal adhesions and excited with the 515-nm laser line to bleach the Venus channel. Both a prebleach image and a postbleach image of the mTFP and Venus channels were acquired, and FRET efficiency was determined by the Leica software (LAS AF). For FRET SE, cells were changed to bicarbonate-free medium containing 10% serum. Images were zoomed three times to focus on single cells and taken at ~2 s/frame for 200 frames or imaged for 10 frames every 30 min for a total length of 180 min at zoom 1×.

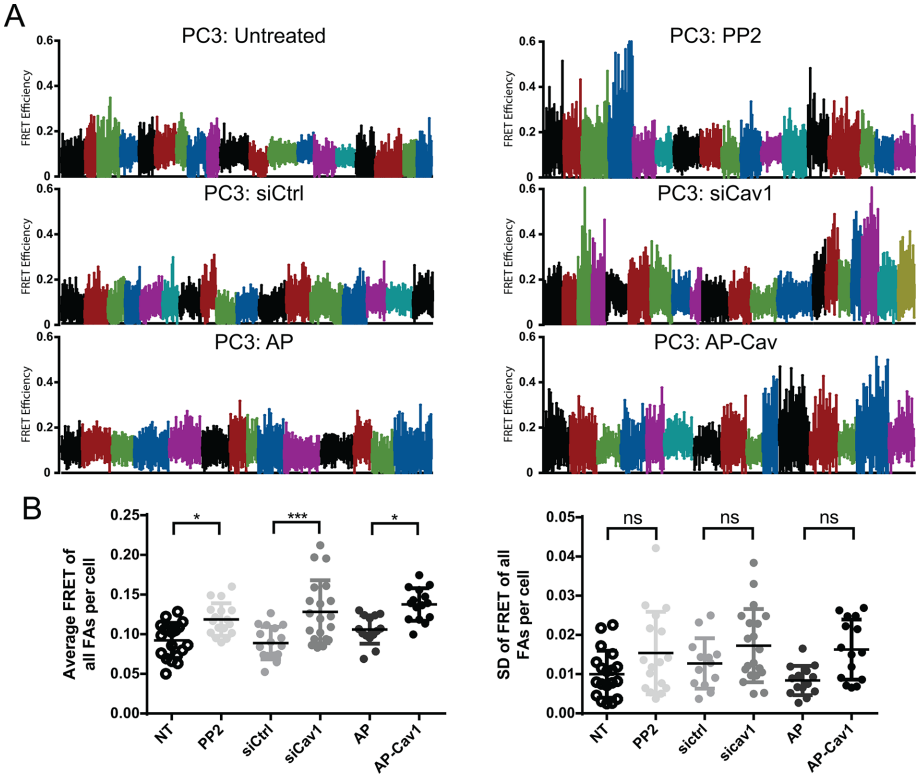

FIGURE 8: pY14Cav1-dependent vinculin tension control is cell specific. (A) The ranges of focal adhesion FRET over the 6.5-min live-cell FRET analysis for PP2, siCtl/siCav1, and AP/AP-Cav treated cell color coded for individual cells. (B) Average and SD of FRET for all the focal adhesions within a cell (cellular FRET). Two-way ANOVA with Bonferroni's multicomparison test; *$p < 0.05$; ***$p < 0.001$; ns, not significant. The absence of significant differences in SD between focal adhesions in individual cells is indicative of synchronous changes between tension levels of focal adhesions within a cell.

Migration assay and cytotoxicity assay

For the Transwell migration assay, cells were trypsinized, counted, and transferred to uncoated 8-μm cell culture inserts (BD Falcon) in medium containing 2% serum; the assembly was placed into 24-well plates containing complete medium with 10% serum. After 16 h, nonmigrated cells were removed from the top of the filter with a cotton swab, and migrated cells on the bottom of the filter were fixed with 3% PFA and stained with 5% crystal violet, and labeled cells were counted. Cell counts were normalized to the control DU145 group. Alternatively, after 2 h, medium in the inserts was replaced with serum-free medium containing 10 μM AP or AP-Cav, and after 6 h, the nonmigrated cells were removed and migrated cells were fixed, stained, and counted. Cell counts were normalized to the DU145 plus AP treatment group. For the cytotoxicity assay, cells were trypsinized, counted, and plated in complete medium for 24 h, which was replaced with serum-free medium (control) or serum-free medium containing 10 μM AP or AP-Cav for 6 h, after which the cells were fixed, stained, counted, and normalized to the control group for each cell line.

GST pull-down and proteomics analysis

The amino acid 1–101 fragments of Cav1 (wild-type, Y14F, Y14D) were subcloned into pGEX-4T1 plasmid (GE Healthcare). GST, GST-Cav1Y14D, and GST-Y14F plasmids were transformed into BL21 *Escherichia coli* strain, and sequence-verified clones were induced with 0.4 mM isopropyl-β-D-thiogalactoside 30°C for 3 h. Beads were prepared using Glutathione-*S*-Sepharose (GE Healthcare) following supplied protocol, and prepared beads (validated by SDS–PAGE and GST, Cav1 Western blots) were stored at 4°C for further use.

Pull-down assays with GST, GST-Cav1Y14D, and GST-Cav1Y14F beads were performed following protocol (Garcia-Carden *et al.*, 1997). Briefly, ~15 μg of total protein lysate was incubated with the GST, GST-Cav1Y14D, or GST-Cav1Y14F beads on rotor at 4°C for 3 h, washed, and subjected to thrombin cleavage (0.1 U/reaction) in reaction buffer (20 mM Tris-HCl, pH 8.0, 100 mM NaCl, 0.3 mM $CaCl_2$, 1 mM DTT, and 0.1% Triton X-100). Reaction mixtures were incubated overnight at 4°C. The supernatant was collected and subjected to quantitative proteomics analysis using formaldehyde labeling. We labeled elution from GST-Cav1Y14D pull down with CH_2O (light), GST-Cav1Y14F pull down with CD_2O (medium), and the GST alone pull down with $^{13}CD_2O$ (heavy) formaldehydes, which gave +28-, +32-, and +36-Da mass shift to the peptides, respectively.

The peptide mixtures were analyzed on an Orbitrap Velos as described (Imami *et al.*, 2013), and the mass spectra were used to identify and quantify proteins using the MaxQuant package (Cox and Mann, 2008). Proteins having at least two peptides were considered for further bioinformatics analysis using the Quantitative Proteomics P-value Calculator (Chen *et al.*, 2014). A distribution-free permutation method based on replicated log(ratio) was applied to the raw peptide ratios to identify significantly altered proteins. Of the significantly changed proteins, only those with a fold change greater >1.5 were considered further.

ACKNOWLEDGMENTS

We thank Kyung-Mee Moon and Nikolay Stoynov for mass spectrometry assistance. This study was supported by grants from the Canadian Institutes for Health Research (CIHR MOP-126029) and Prostate Cancer Canada, as well as a China Scholarship Council-UBC Doctoral Scholarship (F.M.). The microscopy (LSI Imaging) and mass spectrometry infrastructure used in this study was supported by the Canada Foundation for Innovation, the British Columbia (BC) Knowledge Development Fund, and, for the latter, the BC Proteomics Network.

REFERENCES

Ariotti N, Rae J, Leneva N, Ferguson C, Loo D, Okano S, Hill MM, Walser P, Collins BM, Parton RG (2015). Molecular characterization of caveolin-induced membrane curvature. J Biol Chem 290, 24875–24890.

Bakolitsa C, Cohen DM, Bankston LA, Bobkov AA, Cadwell GW, Jennings L, Critchley DR, Craig SW, Liddington RC (2004). Structural basis for vinculin activation at sites of cell adhesion. Nature 430, 583–586.

Balaban NQ, Schwarz US, Riveline D, Goichberg P, Tzur G, Sabanay I, Mahalu D, Safran S, Bershadsky A, Addadi L, Geiger B (2001). Force and focal adhesion assembly: a close relationship studied using elastic micropatterned substrates. Nat Cell Biol 3, 466–472.

Beardsley A, Fang K, Mertz H, Castranova V, Friend S, Liu J (2005). Loss of caveolin-1 polarity impedes endothelial cell polarization and directional movement. J Biol Chem 280, 3541–3547.
Bernatchez PN, Bauer PM, Yu J, Prendergast JS, He P, Sessa WC (2005). Dissecting the molecular control of endothelial NO synthase by caveolin-1 using cell-permeable peptides. Proc Natl Acad Sci USA 102, 761–766.
Boscher C, Nabi IR (2013). Galectin-3- and phospho-caveolin-1-dependent outside-in integrin signaling mediates the EGF motogenic response in mammary cancer cells. Mol Biol Cell 24, 2134–2145.
Bucci M, Gratton JP, Rudic RD, Acevedo L, Roviezzo F, Cirino G, Sessa WC (2000). In vivo delivery of the caveolin-1 scaffolding domain inhibits nitric oxide synthesis and reduces inflammation. Nat Med 6, 1362–1367.
Burridge K, Fath K, Kelly T, Nuckolls G, Turner C (1988). Focal adhesions: transmembrane junctions between the extracellular matrix and the cytoskeleton. Annu Rev Cell Biol 4, 487–525.
Burridge K, Guilluy C (2016). Focal adhesions, stress fibers and mechanical tension. Exp Cell Res 343, 14–20.
Byrne DP, Dart C, Rigden DJ (2012). Evaluating caveolin interactions: do proteins interact with the caveolin scaffolding domain through a widespread aromatic residue-rich motif? PLoS One 7, e44879.
Carisey A, Tsang R, Greiner AM, Nijenhuis N, Heath N, Nazgiewicz A, Kemkemer R, Derby B, Spatz J, Ballestrem C (2013). Vinculin regulates the recruitment and release of core focal adhesion proteins in a force-dependent manner. Curr Biol 23, 271–281.
Case LB, Waterman CM (2015). Integration of actin dynamics and cell adhesion by a three-dimensional, mechanosensitive molecular clutch. Nat Cell Biol 17, 955–963.
Chan CE, Odde DJ (2008). Traction dynamics of filopodia on compliant substrates. Science 322, 1687–1691.
Chen D, Shah A, Nguyen H, Loo D, Inder KL, Hill MM (2014). Online quantitative proteomics p-value calculator for permutation-based statistical testing of peptide ratios. J Proteome Res 13, 4184–4191.
Chen Z, Bakhshi FR, Shajahan AN, Sharma T, Mao M, Trane A, Bernatchez P, van Nieuw Amerongen GP, Bonini MG, Skidgel RA, *et al.* (2012). Nitric oxide-dependent Src activation and resultant caveolin-1 phosphorylation promote eNOS/caveolin-1 binding and eNOS inhibition. Mol Biol Cell 23, 1388–1398.
Cohen DM, Kutscher B, Chen H, Murphy DB, Craig SW (2006). A conformational switch in vinculin drives formation and dynamics of a talin-vinculin complex at focal adhesions. J Biol Chem 281, 16006–16015.
Collins BM, Davis MJ, Hancock JF, Parton RG (2012). Structure-based reassessment of the caveolin signaling model: do caveolae regulate signaling through caveolin-protein interactions? Dev Cell 23, 11–20.
Couet J, Li S, Okamoto T, Ikezu T, Lisanti MP (1997). Identification of peptide and protein ligands for the caveolin-scaffolding domain. Implications for the interaction of caveolin with caveolae-associated proteins. J Biol Chem 272, 6525–6533.
Cox J, Mann M (2008). MaxQuant enables high peptide identification rates, individualized p.p.b.-range mass accuracies and proteome-wide protein quantification. Nat Biotechnol 26, 1367–1372.
del Pozo MA, Balasubramanian N, Alderson NB, Kiosses WB, Grande-Garcia A, Anderson RG, Schwartz MA (2005). Phospho-caveolin-1 mediates integrin-regulated membrane domain internalization. Nat Cell Biol 7, 901–908.
del Rio A, Perez-Jimenez R, Liu R, Roca-Cusachs P, Fernandez JM, Sheetz MP (2009). Stretching single talin rod molecules activates vinculin binding. Science 323, 638–641.
El-Gendi SM, Mostafa MF, El-Gendi AM (2012). Stromal caveolin-1 expression in breast carcinoma. Correlation with early tumor recurrence and clinical outcome. Pathol Oncol Res 18, 459–469.
Garcia-Cardena G, Martasek P, Masters BS, Skidd PM, Couet J, Li S, Lisanti MP, Sessa WC (1997). Dissecting the interaction between nitric oxide synthase (NOS) and caveolin. Functional significance of the nos caveolin binding domain in vivo. J Biol Chem 272, 25437–25440.
Gardel ML, Schneider IC, Aratyn-Schaus Y, Waterman CM (2010). Mechanical integration of actin and adhesion dynamics in cell migration. Annu Rev Cell Dev Biol 26, 315–333.
Gaus K, Le Lay S, Balasubramanian N, Schwartz MA (2006). Integrin-mediated adhesion regulates membrane order. J Cell Biol 174, 725–734.
Glenney JR Jr (1989). Tyrosine phosphorylation of a 22-kDa protein is correlated with transformation by Rous sarcoma virus. J Biol Chem 264, 20163–20166.
Goetz JG, Joshi B, Lajoie P, Strugnell SS, Scudamore T, Kojic LD, Nabi IR (2008a). Concerted regulation of focal adhesion dynamics by galectin-3 and tyrosine-phosphorylated caveolin-1. J Cell Biol 180, 1261–1275.
Goetz JG, Lajoie P, Wiseman SM, Nabi IR (2008b). Caveolin-1 in tumor progression: the good, the bad and the ugly. Cancer Metastasis Rev 27, 715–735.
Gould ML, Williams G, Nicholson HD (2010). Changes in caveolae, caveolin, and polymerase 1 and transcript release factor (PTRF) expression in prostate cancer progression. Prostate 70, 1609–1621.
Grande-Garcia A, Echarri A, de Rooij J, Alderson NB, Waterman-Storer CM, Valdivielso JM, del Pozo MA (2007). Caveolin-1 regulates cell polarization and directional migration through Src kinase and Rho GTPases. J Cell Biol 177, 683–694.
Grashoff C, Hoffman BD, Brenner MD, Zhou R, Parsons M, Yang MT, McLean MA, Sligar SG, Chen CS, Ha T, Schwartz MA (2010). Measuring mechanical tension across vinculin reveals regulation of focal adhesion dynamics. Nature 466, 263–266.
Gratton JP, Lin MI, Yu J, Weiss ED, Jiang ZL, Fairchild TA, Iwakiri Y, Groszmann R, Claffey KP, Cheng YC, Sessa WC (2003). Selective inhibition of tumor microvascular permeability by cavtratin blocks tumor progression in mice. Cancer Cell 4, 31–39.
Hamadi A, Bouali M, Dontenwill M, Stoeckel H, Takeda K, Ronde P (2005). Regulation of focal adhesion dynamics and disassembly by phosphorylation of FAK at tyrosine 397. J Cell Sci 118, 4415–4425.
Hernandez-Varas P, Berge U, Lock JG, Stromblad S (2015). A plastic relationship between vinculin-mediated tension and adhesion complex area defines adhesion size and lifetime. Nat Commun 6, 7524.
Hill MM, Scherbakov N, Schiefermeier N, Baran J, Hancock JF, Huber LA, Parton RG, Parat MO (2007). Reassessing the role of phosphocaveolin-1 in cell adhesion and migration. Traffic 8, 1695–1705.
Hoffman BD (2014). The detection and role of molecular tension in focal adhesion dynamics. Prog Mol Biol Transl Sci 126, 3–24.
Hoffmann C, Berking A, Agerer F, Buntru A, Neske F, Chhatwal GS, Ohlsen K, Hauck CR (2010). Caveolin limits membrane microdomain mobility and integrin-mediated uptake of fibronectin-binding pathogens. J Cell Sci 123, 4280–4291.
Hoop CL, Sivanandam VN, Kodali R, Srnec MN, van der Wel PC (2012). Structural characterization of the caveolin scaffolding domain in association with cholesterol-rich membranes. Biochemistry 51, 90–99.
Huang Y, Day RN, Gunst SJ (2014). Vinculin phosphorylation at Tyr1065 regulates vinculin conformation and tension development in airway smooth muscle tissues. J Biol Chem 289, 3677–3688.
Humphries JD, Wang P, Streuli C, Geiger B, Humphries MJ, Ballestrem C (2007). Vinculin controls focal adhesion formation by direct interactions with talin and actin. J Cell Biol 179, 1043–1057.
Imami K, Bhavsar AP, Yu H, Brown NF, Rogers LD, Finlay BB, Foster LJ (2013). Global impact of Salmonella pathogenicity island 2-secreted effectors on the host phosphoproteome. Mol Cell Proteomics 12, 1632–1643.
Joshi B, Bastiani M, Strugnell SS, Boscher C, Parton RG, Nabi IR (2012). Phosphocaveolin-1 is a mechanotransducer that induces caveola biogenesis via Egr1 transcriptional regulation. J Cell Biol 199, 425–435.
Joshi B, Strugnell SS, Goetz JG, Kojic LD, Cox ME, Griffith OL, Chan SK, Jones SJ, Leung SP, Masoudi H, Leung S, Wiseman SM, Nabi IR (2008). Phosphorylated caveolin-1 regulates Rho/ROCK-dependent focal adhesion dynamics and tumor cell migration and invasion. Cancer Res 68, 8210–8220.
Kanchanawong P, Shtengel G, Pasapera AM, Ramko EB, Davidson MW, Hess HF, Waterman CM (2010). Nanoscale architecture of integrin-based cell adhesions. Nature 468, 580–584.
Kraning-Rush CM, Califano JP, Reinhart-King CA (2012). Cellular traction stresses increase with increasing metastatic potential. PLoS One 7, e32572.
Lajoie P, Partridge EA, Guay G, Goetz JG, Pawling J, Lagana A, Joshi B, Dennis JW, Nabi IR (2007). Plasma membrane domain organization regulates EGFR signaling in tumor cells. J Cell Biol 179, 341–356.
Lee H, Volonte D, Galbiati F, Iyengar P, Lublin DM, Bregman DB, Wilson MT, Campos-Gonzalez R, Bouzahzah B, Pestell RG, *et al.* (2000). Constitutive and growth factor-regulated phosphorylation of caveolin-1 occurs at the same site (Tyr-14) in vivo: identification of a c-Src/Cav-1/Grb7 signaling cassette. Mol Endocrinol 14, 1750–1775.
Levental KR, Yu H, Kass L, Lakins JN, Egeblad M, Erler JT, Fong SF, Csiszar K, Giaccia A, Weninger W,, *et al.* (2009). Matrix crosslinking forces tumor progression by enhancing integrin signaling. Cell 139, 891–906.
Li S, Couet J, Lisanti MP (1996). Src tyrosine kinases, Galpha subunits, and H-Ras share a common membrane-anchored scaffolding protein, caveolin. Caveolin binding negatively regulates the auto-activation of Src tyrosine kinases. J Biol Chem 271, 29182–29190.

Li S, Okamoto T, Chun M, Sargiacomo M, Casanova JE, Hansen SH, Nishimoto I, Lisanti MP (1995). Evidence for a regulated interaction between heterotrimeric G proteins and caveolin. J Biol Chem 270, 15693–15701.
Margadant F, Chew LL, Hu X, Yu H, Bate N, Zhang X, Sheetz M (2011). Mechanotransduction in vivo by repeated talin stretch-relaxation events depends upon vinculin. PLOS Biol 9, e1001223.
Meng F, Joshi B, Nabi IR (2015). Galectin-3 overrides PTRF/cavin-1 reduction of PC3 prostate cancer cell migration. PLoS One 10, e0126056.
Mitchison T, Kirschner M (1988). Cytoskeletal dynamics and nerve growth. Neuron 1, 761–772.
Mitra SK, Schlaepfer DD (2006). Integrin-regulated FAK-Src signaling in normal and cancer cells. Curr Opin Cell Biol 18, 516–523.
Nethe M, Anthony EC, Fernandez-Borja M, Dee R, Geerts D, Hensbergen PJ, Deelder AM, Schmidt G, Hordijk PL (2010). Focal-adhesion targeting links caveolin-1 to a Rac1-degradation pathway. J Cell Sci 123, 1948–1958.
Nomura R, Fujimoto T (1999). Tyrosine-phosphorylated caveolin-1: immunolocalization and molecular characterization. Mol Biol Cell 10, 975–986.
Nystrom FH, Chen H, Cong LN, Li Y, Quon MJ (1999). Caveolin-1 interacts with the insulin receptor and can differentially modulate insulin signaling in transfected Cos-7 cells and rat adipose cells. Mol Endocrinol 13, 2013–2024.
Okamoto T, Schlegel A, Scherer PE, Lisanti MP (1998). Caveolins, a family of scaffolding proteins for organizing preassembled signaling complexes at the plasma membrane. J Biol Chem 273, 5419–5422.
Ortiz R, Diaz J, Diaz N, Lobos-Gonzalez L, Cardenas A, Contreras P, Diaz MI, Otte E, Cooper-White J, Torres V,, *et al*. (2016). Extracellular matrix-specific Caveolin-1 phosphorylation on tyrosine 14 is linked to augmented melanoma metastasis but not tumorigenesis. Oncotarget 7, 40571–40593.
Parat MO, Anand-Apte B, Fox PL (2003). Differential caveolin-1 polarization in endothelial cells during migration in two and three dimensions. Mol Biol Cell 14, 3156–3168.
Parton RG, del Pozo MA (2013). Caveolae as plasma membrane sensors, protectors and organizers. Nat Rev 14, 98–112.
Paszek MJ, Zahir N, Johnson KR, Lakins JN, Rozenberg GI, Gefen A, Reinhart-King CA, Margulies SS, Dembo M, Boettiger D, *et al*. (2005). Tensional homeostasis and the malignant phenotype. Cancer Cell 8, 241–254.
Place AT, Chen Z, Bakhshi FR, Liu G, O'Bryan JP, Minshall RD (2011). Cooperative role of caveolin-1 and C-terminal Src kinase binding protein in C-terminal Src kinase-mediated negative regulation of c-Src. Mol Pharmacol 80, 665–672.
Plotnikov SV, Pasapera AM, Sabass B, Waterman CM (2012). Force fluctuations within focal adhesions mediate ECM-rigidity sensing to guide directed cell migration. Cell 151, 1513–1527.
Provenzano PP, Eliceiri KW, Campbell JM, Inman DR, White JG, Keely PJ (2006). Collagen reorganization at the tumor-stromal interface facilitates local invasion. BMC Med 4, 38.
Radel C, Rizzo V (2005). Integrin mechanotransduction stimulates caveolin-1 phosphorylation and recruitment of Csk to mediate actin reorganization. Am J Physiol Heart Circ Physiol 288, H936–H945.
Salanueva IJ, Cerezo A, Guadamillas MC, del Pozo MA (2007). Integrin regulation of caveolin function. J Cell Mol Med 11, 969–980.
Satoh T, Yang G, Egawa S, Addai J, Frolov A, Kuwao S, Timme TL, Baba S, Thompson TC (2003). Caveolin-1 expression is a predictor of recurrence-free survival in pT2N0 prostate carcinoma diagnosed in Japanese patients. Cancer 97, 1225–1233.
Shajahan AN, Dobbin ZC, Hickman FE, Dakshanamurthy S, Clarke R (2012). Tyrosine-phosphorylated caveolin-1 (Tyr-14) increases sensitivity to paclitaxel by inhibiting BCL2 and BCLxL proteins via c-Jun N-terminal kinase (JNK). J Biol Chem 287, 17682–17692.
Sinha B, Koster D, Ruez R, Gonnord P, Bastiani M, Abankwa D, Stan RV, Butler-Browne G, Vedie B, Johannes L, *et al*. (2010). Cells respond to mechanical stress by rapid disassembly of caveolae. Cell 144, 402–413.
Sloan EK, Ciocca DR, Pouliot N, Natoli A, Restall C, Henderson MA, Fanelli MA, Cuello-Carrion FD, Gago FE, Anderson RL (2009). Stromal cell expression of caveolin-1 predicts outcome in breast cancer. Am J Pathol 174, 2035–2043.
Sverdlov M, Shinin V, Place AT, Castellon M, Minshall RD (2009). Filamin A regulates caveolae internalization and trafficking in endothelial cells. Mol Biol Cell 20, 4531–4540.
Thievessen I, Thompson PM, Berlemont S, Plevock KM, Plotnikov SV, Zemljic-Harpf A, Ross RS, Davidson MW, Danuser G, Campbell SL, Waterman CM (2013). Vinculin–actin interaction couples actin retrograde flow to focal adhesions, but is dispensable for focal adhesion growth. J Cell Biol 202, 163.
Trane AE, Pavlov D, Sharma A, Saqib U, Lau K, van Petegem F, Minshall RD, Roman LJ, Bernatchez PN (2014). Deciphering the binding of caveolin-1 to client protein endothelial nitric-oxide synthase (eNOS): scaffolding subdomain identification, interaction modeling, and biological significance. J Biol Chem 289, 13273–13283.
Ursin G, Hovanessian-Larsen L, Parisky YR, Pike MC, Wu AH (2005). Greatly increased occurrence of breast cancers in areas of mammographically dense tissue. Breast Cancer Res 7, R605–R608.
Wary KK, Mariotti A, Zurzolo C, Giancotti FG (1998). A requirement for caveolin-1 and associated kinase Fyn in integrin signaling and anchorage-dependent cell growth. Cell 94, 625–634.
Webb DJ, Donais K, Whitmore LA, Thomas SM, Turner CE, Parsons JT, Horwitz AF (2004). FAK-Src signalling through paxillin, ERK and MLCK regulates adhesion disassembly. Nat Cell Biol 6, 154–161.
Williams TM, Lisanti MP (2005). Caveolin-1 in oncogenic transformation, cancer, and metastasis. Am J Physiol Cell Physiol 288, C494–C506.
Yang G, Truong LD, Wheeler TM, Thompson TC (1999). Caveolin-1 expression in clinically confined human prostate cancer: a novel prognostic marker. Cancer Res 59, 5719–5723.
Zhang Z, Izaguirre G, Lin SY, Lee HY, Schaefer E, Haimovich B (2004). The phosphorylation of vinculin on tyrosine residues 100 and 1065, mediated by SRC kinases, affects cell spreading. Mol Biol Cell 15, 4234–4247.
Ziegler WH, Liddington RC, Critchley DR (2006). The structure and regulation of vinculin. Trends Cell Biol 16, 453–460.
Zimnicka AM, Husain YS, Shajahan AN, Sverdlov M, Chaga O, Chen Z, Toth PT, Klomp J, Karginov AV, Tiruppathi C, *et al*. (2016). Src-dependent phosphorylation of caveolin-1 Tyr14 promotes swelling and release of caveolae. Mol Biol Cell 27, 2090–2106.